2025 IEEE International Conference on Systems, Man, and Cybernetics (SMC)
October 5-8, 2025. Vienna, Austria

Event-Triggered Control for Autonomous Detection and Treatment of Membrane Lesions using Microrobot Swarms

Yun Gao, Hao Gao, Ziming Wang, Yang Shi, and Yiding Ji†

2025 IEEE International Conference on Systems, Man, and Cybernetics (SMC) | 979-8-3315-3358-8/25/$31.00 ©2025 IEEE | DOI: 10.1109/SMC58881.2025.11343544

***Abstract*— Recent advances in robotics have expanded the potential of microrobot swarms (MRSs) in medicine, yet clinical deployment remains limited due to reliance on non-autonomous systems. This study proposes an event-triggered distributed coverage control framework that enables MRSs to autonomously detect and treat membrane lesions. To model lesion dynamics accurately, we introduce a coupled reaction-diffusion equation and a Hawkes process that capture spatial spread and temporal emergence. This model informs a modified Lloyd algorithm to guide MRSs toward the centroids of Voronoi cells, optimizing drug release over pre-existing lesion areas. Furthermore, we design an event-triggered mechanism prioritizing treatment of newly emerging lesions, redirecting microrobots to lesion centers for prioritized response. This adaptive framework effectively addresses lesion proliferation and promotes membrane healing. Simulations demonstrate improved coverage efficiency and lesion containment compared to conventional strategies.**

***Index Terms*— Microrobot swarms, coverage control, medical event-triggered control, autonomous detection, drug delivery.**

I. Introduction

Robotics is undergoing a revolutionary phase characterized by miniaturization, driving innovative applications in medicine [1], [2]. Microrobot swarms (MRSs) have emerged as a promising technology, demonstrating the capacity to autonomously identify and precisely treat pathological lesions that require extensive human intervention. Each microrobot within the swarm is equipped with sensors and actuators that facilitate autonomous navigation to lesions and delivery of drugs [3]. This advancement aligns with the growing demand for complex yet minimally invasive medical interventions, offering viable treatment options for conditions deemed intractable. The deployment of MRSs in medical procedures signifies a shift away from the discomfort and invasiveness of traditional monitoring and treatment methods [4], indicating a new era of patient-centered and precise healthcare [5].

Membrane lesions usually deteriorate structures such as the mucosal layer, peritoneum, and Glisson capsule, causing chronic conditions that require prompt intervention. If not properly treated, these lesions lead to severe complications such as tissue perforation and hemorrhage [6]. Conventional therapeutic approaches, including oral medications and intravenous infusions, often have limited efficacy, as they do not directly target the lesions [7]. The lack of sustained control mechanisms in traditional therapies frequently results in recurrent episodes of the condition [8]. Consequently, the application of MRSs for the detection and treatment of lesions is of substantial clinical significance.

Despite the potential of microrobots in therapeutic applications, current research is still in its early stages [9]. A notable limitation is the focus on the individual microrobot for treatment, which is inadequate for treating densely distributed or dynamically changing membrane lesions. Although swarm-based approaches have been explored, these systems often lack autonomous propulsion and depend on bodily fluid flow or external magnetic fields for movement [10], restricting their practical applicability. Some machine learning techniques have been proposed, yet there remains a significant gap in understanding the specific mechanisms governing robot movement at lesion sites, which frequently raises stability concerns [11]. Overall, existing methods suffer from notable drawbacks for clinical applications.

To overcome the above limitations, we propose an event-triggered control [12]–[15] approach that empowers MRSs to autonomously detect and treat membrane lesions. This framework comprises two mechanisms: a spatial coverage strategy tailored to lesion distribution, and a lesion-aware reactive control strategy triggered by pathological events. First, inspired by spatial division-based coverage control [16]–[18], we improve traditional coverage strategies by employing an enhanced centroidal Voronoi tessellation (CVT) guided by pathogen distribution and further refined through a membrane lesions model, making the coverage process more consistent with biological response mechanisms.

However, due to environmental changes, microbial community diffusion, *etc.*, using only coverage control in medical scenarios still has limitations [19]. To address the dynamic nature of lesion development, we argue that timely intervention targeting newly emerging lesions is essential to prevent the escalation of inflammation. Therefore, we leverage event-triggered control to establish a set of identification criteria and a corresponding control strategy that prioritizes treatment and enables real-time response coordination. Through the integration of two complementary lesion management strategies, our framework effectively suppresses the spread of chronic pathological regions, thereby enhancing both coverage efficiency and therapeutic effectiveness. Our main contributions are summarized as follows:

Yun Gao, Hao Gao, Ziming Wang, and Yiding Ji are with Robotics and Autonomous Systems Thrust, Systems Hub, Hong Kong University of Science and Technology (Guangzhou), Guangzhou, China. Emails: y.gao@gaoyunailab.com, ghalfred39@gmail.com, wwwangziming@163.com, jiyiding@hkust-gz.edu.cn.

Yang Shi is with the Department of Mechanical Engineering, Faculty of Engineering, University of Victoria, Victoria, Canada. Email: yshi@uvic.ca.

†Corresponding author.

Financial support: National Natural Science Foundation of China grants 62303389, 62373289; Guangdong Basic and Applied Basic Research Funding grants 2022A151511076, 2024A1515012586; Guangdong Scientific Research Platform and Project Scheme grant 2024KTSCX039; Guangzhou-HKUST(GZ) Joint Funding Program grants 2024A03J0618, 2024A03J0680.

- This study proposes a novel framework of medical intervention that enables autonomous lesion detection and targeted drug delivery, overcoming the limitations of existing approaches that predominantly rely on externally actuated microrobots—such as those driven by magnetic fields and inherently lacking autonomous mobility.
- This study introduces a reaction-diffusion equation and a Hawkes process to model membrane lesions, which are employed to improve the Lloyd algorithm-based coverage control strategy and enhance its clinical applicability. Our model guides microrobots towards the centroids of their Voronoi cells to release therapeutic agents, allowing efficient management of pre-existing lesion areas.
- An event-triggered control strategy is developed for microrobots to preferentially respond to newly emerging lesions. This approach contributes to faster and more effective treatment by suppressing the spread of pathological sites.

The remainder of this paper is organized as follows. Section II introduces the models of membrane lesions and MRSs, and formulates the problem of autonomous detection and targeted treatment. Section III presents an event-triggered control approach that enables microrobots to perform this task autonomously. Section IV provides simulation results to demonstrate the performance of our method and compare it with some existing ones. Finally, Section V wraps up the paper and outlines potential future research directions.

II. Preliminaries and Problem Formulation

A. Model of Membrane Lesions

In this study, the task environment is a relatively flat membrane regarded as a compact convex two-dimensional plane $\mathcal{Q} \subset \mathbb{R}^2$. We focus on lesions resulting from auto-inflammatory conditions, such as ulcers on mucosal surfaces, which typically manifest as nearly circular formations. Around these formations, a significant concentration of pathogens (CoP) accumulates, markedly exceeding the healthy membrane. There is a positive correlation between CoP and the severity of lesions. This characteristic enables an accurate identification of lesions' location by analyzing the pathogens' distribution patterns on the membrane.

Let $s_n \in \mathcal{Q}$ denote the center position of the n^{th} lesion. The initial CoP at any point $q \in \mathcal{Q}$ can be computed as:

$$\phi(q,0) = \mu + \textstyle\sum_{n=1}^{N(0)} \gamma_n g(q, s_n), \tag{1}$$

where $\mu \in \mathbb{R}_{>0}$ is the inherent CoP on the membrane when no lesions exist. The variable $N(k) \in \mathbb{Z}_+$ indicates the number of lesions at iteration k and $\gamma_n \in (0,1)$ denotes the peak CoP contribution of the n^{th} lesion. The spatial influence on iteration $k=0$ of the n^{th} lesion, which is centered at s_n and has impact range $\sigma_n(0) \in \mathbb{R}_{>0}$, is given by (2):

$$g(q, s_n) = \frac{1}{\sqrt{2\pi}\sigma_n(0)} e^{\frac{\|q-s_n\|^2}{2\sigma_n^2(0)}}. \tag{2}$$

Under pharmacological intervention, the lesions may no longer follow the Gaussian distribution. Then, we leverage a variant of FitzHugh-Nagumo model [20] to describe the subsequent process by the following reaction-diffusion equation:

$$\frac{\partial \phi(q,k)}{\partial k} - \dot{\sigma}_n(k)\nabla^2\phi(q,k) + F(q, P(k)) = 0, \tag{3}$$

where $\dot{\sigma}_n(k) \in \mathbb{R}_{\geq 0}$ denotes diffusivity of pathogens, and $\nabla^2\phi(q,k)$ is the Laplacian of the concentration field $\phi(q,k)$. The term $F(q,P(k)) \in \mathbb{R}_{\geq 0}$ indicates the influence of MRS on lesions, and $P(k) \in \mathbb{R}^{2\times I}$ denotes the spatial configuration of the MRS. Additional details regarding these configurations are provided in Section II-B.

In particular, the appearance of the lesions is random, which is pivotal for the proposed method to adapt to dynamic environmental changes. Although the appearance of lesions is unpredictable, a reasonable assumption is made:

Assumption 1. *For areas where lesions have been observed, and their adjacent zones, the probability of recurrence of lesions is relatively higher due to abnormal pathogens.*

We then apply the Hawkes process (4) to describe the time and location of the random appearance of the lesions:

$$\xi(s_n,k) = \psi(s_n,k) + \textstyle\sum_k \alpha\rho e^{-\rho(T-kT_s)} g(q, s_n), \tag{4}$$

where $\xi(s_n,k)$ represents the conditional intensity function, which characterizes the instantaneous probability of a lesion occurring at location s_n at iteration k, given the event history. In contrast, $\psi(s_n,k)$ represents the baseline intensity, capturing the inherent likelihood of lesion occurrence at the same spatiotemporal coordinates in the absence of influence from prior lesions. The parameter α controls the intensity of lesion appearance, while ρ governs its temporal decay rate.

B. Model of Microrobot Swarms

An MRS consists of $I \in \mathbb{Z}_+$ microrobots that perform tasks in $\mathcal{Q}$, and the position of each robot is given as $p_i(k) \in \mathbb{R}^2$. The collective configuration of this MRS at moment k is described by the matrix $P(k) = [p_1^T(k), \ldots, p_I^T(k)]^T$. For the sake of simplicity, we ignore the detailed body structure of microrobots and consider them as particles, which is reasonable given their extremely tiny size. The motion of each microrobot is governed by the kinematic equation:

$$p_i(k+1) = p_i(k) + T_s u_i(k), \tag{5}$$

where $u_i(k)$ is the control input bounded by the robot's maximum velocity $v \in \mathbb{R}_{\geq 0}$ and T_s is the sampling time.

Microrobots within the MRS can communicate, monitor lesions, and deliver drugs for treatment. Regarding communication, each robot is capable of establishing bidirectional connections with other microrobots located within a circular area of radius $R_c \in \mathbb{R}_{\geq 0}$, *i.e.*, $\|p_i(k) - p_j(k)\| \leq R_c$. Robots that satisfy these conditions are called the neighbors of the i^{th} robot, *i.e.*, $\mathcal{N}_i(k) = \{j : \|p_i(k) - p_j(k)\| \leq R_c\}$.

These microrobots monitor CoP levels and release therapeutic agents to treat lesions within radius $R_t \in \mathbb{R}_{\geq 0}$. We denote $B(p_i(k), R_t) \in \mathbb{R}_{\geq 0}$ as the influence range of the i^{th} microrobot at iteration k. The therapeutic efficacy exhibits

distance-dependent attenuation, with the treatment effect diminishing as the distance from the microrobot increases and vanishing beyond a radius R_t. To model the therapeutic effect of the i^{th} microrobot on lesions, we employ a continuously differentiable function to model the drug release efficacy:

$$f(q,p_i(k))=\begin{cases}\delta e^{-\lambda\|q-p_i(k)\|^2}-\varrho & q\in B(p_i(k),R_t)\\ 0 & q\notin B(p_i(k),R_t)\end{cases}, \quad (6)$$

where $\delta\in(0,1)$ represents the maximum therapeutic effect for CoP clearance, $\lambda\in(0,\infty)$ is the attenuation parameter, and $\varrho=\delta e^{-\lambda R_i^2}$ ensures the function vanishes at the boundary. The overall therapeutic effect is given by:

$$F(q,P(k))=\sum_{i=1}^{I}\beta f(q,p_i(k)), \quad (7)$$

where $\beta\in\{0,1\}$ is the activation indicator. When $q\in B(p_i(k),R_t)$, $\beta=1$; when $q\notin B(p_i(k),R_t)$, $\beta=0$.

C. Problem Formulation

In this work, the membrane is modeled as a two-dimensional convex compact region $\mathcal{Q}$. A varying number $N(k)$ of lesions appear on the membrane, where their appearance follows the Hawkes process (4) and their concentration diffusion mechanism follows the reaction-diffusion equation (3). Then the key problem is formulated below:

Problem 1 (Autonomous detection and treatment of lesions)**.** *Given a team of I microrobots deployed in $\mathcal{Q}$, they have a limited communication range R_c, monitoring/treatment range R_t and therapeutic capacity given by* (6)*. These microrobots start from $P(0)$ to explore the task membrane and their kinetics are governed by* (5)*. Our objective is to design a control strategy that enables microrobots to monitor real-time CoP levels to detect lesions and deliver drugs for subsequent treatment, thus improving clinical efficiency.*

III. Event-Triggered Control Scheme

A. Solution Overview

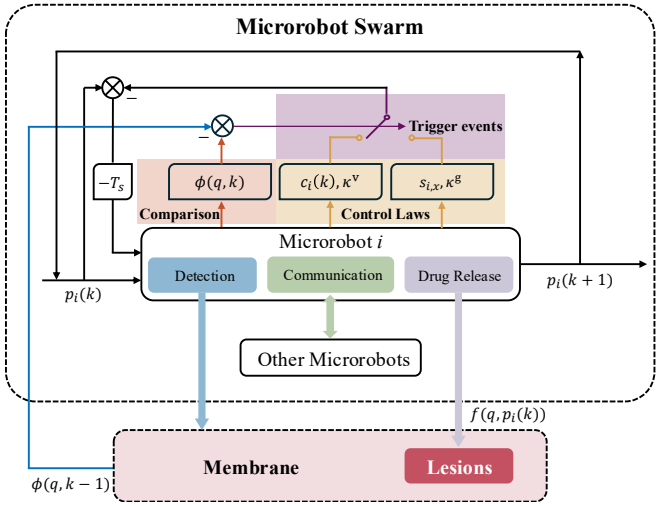

Fig. 1: The autonomous detection and target treatment framework.

The proposed framework in Fig. 1 begins by directing the robots towards the centroid of their Voronoi tessellation to maximize drug coverage, where the initial concentration of pathogens (CoP) level determines the partition. Meanwhile, the CoP distribution on the membrane is monitored for emerging lesions. Once detected, the robots are relocated to the center of emerging lesions to deliver drugs for treatment, effectively controlling the spread of lesions.

B. Detection and Treatment of Existing Lesions

In this section, the proposed control strategy operates as follows: the MRS first partitions the membrane into Voronoi tessellations based on initial robot positions, as defined in (8). Each microrobot continuously monitors the CoP distribution within its Voronoi cell and autonomously navigates to the centroids while releasing therapeutic agents to treat lesions. The update continues until $\forall q\in\mathcal{Q}$ such that $\phi(q,k)=\mu$.

$$V_i(k)=\{q\in\mathcal{Q}\,|\,\|q-p_i(k)\|\le\|q-p_j(k)\|,\forall j\neq i\}. \quad (8)$$

To maximize therapeutic effectiveness, we aim to achieve the greatest CoP reduction at each iteration. We define the CoP change as $\Delta\phi(q,k)=-f(q,p_i(k))\phi(q,k)$. The global CoP change across the entire membrane is then given by:

$$\mathcal{H}_1(P(k),k)=\sum_{i=1}^{I}\int_{V_i(k)}f(q,p_i(k))\phi(q,k)dq. \quad (9)$$

Our objective is to maximize $\mathcal{H}_1(P(k),k)$. Using gradient-based optimization, we can obtain:

$$\frac{\partial\mathcal{H}_1(P(k),k)}{\partial p_i(k)}=-m_i(k)(p_i(k)-c_i(k)), \quad (10)$$

where $m_i(k)=2\lambda\int_{V_i(k)}f(q,p_i(k))\phi(q,k)dq$ and $c_i(k)=2\lambda m_i^{-1}(k)\int_{V_i(k)}f(q,p_i(k))\phi(q,k)qdq$ denote the mass and centroid of Voronoi cell $V_i(k)$, respectively. The solution requires $\partial\mathcal{H}_1(P(k),k)/\partial p_i(k)=0$, yielding $p_i(k)=c_i(k)$. Based on this optimal policy, we define Lyapunov function $L(q,k)=\sum_{i=1}^{I}\|p_i(k)-c_i(k)\|^2$ and proceed to compute its overall rate of change over time:

$$\frac{dL(q,k)}{dk}=(P(k)-C(k))^T((E_{2I}-\frac{\partial C(k)}{\partial P(k)})\dot{P}(k)-\dot{C}(k)), \quad (11)$$

where $E_{2I}\in\mathbb{R}^{2I\times 2I}$ stands for the identity matrix, $C(k)=[c_1^T(k),\dots,c_i^T(k)]^T$. To enforce a negative change rate, we design the control law as follows:

$$U^{\mathrm{v}}(k)=-(E_{2I}-\frac{\partial C(k)}{\partial P(k)})^{-1}(\kappa^{\mathrm{v}}(P(k)-C(k))-\dot{C}(k)), \quad (12)$$

where $U^{\mathrm{v}}(k)=[(u_1^{\mathrm{v}}(k))^T,\dots,(u_I^{\mathrm{v}}(k))^T]^T$, $\kappa^{\mathrm{v}}\in\mathbb{R}_{>0}$ is the control gain. However, the presence of inverse operations renders the control law centralized, as it prevents the decoupling of individual control components $u_i^{\mathrm{v}}(k)$ from the global vector $U^{\mathrm{v}}(k)$. To address this issue, we introduce a preconditioned Neumann series to approximate the inverse term $(E_{2I}-\partial C(k)/\partial P(k))^{-1}$, which facilitates the design of a distributed control law as follows:

$$u_i^{\mathrm{v}}(k)=-\kappa^{\mathrm{v}}(p_i(k)-c_i(k))+\dot{c}_i(k)-\Omega_{ij}(k), \quad (13)$$

where $\Omega_{ij}(k)$ is a compensation item that involving $J_{ii}(k)=\partial c_i(k)/\partial p_i(k)$, $J_{ij}(k)=\partial c_i(k)/\partial p_j(k)$, and $\dot{c}_j(k)$, whose explicit forms are given below:

$$\Omega_{ij}(k)=(E_2-J_{ii}(k))\sum_j J_{ij}(k)(\kappa^{\mathrm{v}}(p_j(k)-c_j(k))-\dot{c}_j(k)), \quad (14)$$

$$J_{ii}(k)=\frac{1}{m_i(k)}\sum_l\int_{\partial V_{il}}\frac{(q-c_i(k))(q-p_i(k))^T\phi(q,k)}{\|p_i(k)-p_l(k)\|}dq, \quad (15)$$

$$J_{ij}(k)=\frac{-1}{m_i(k)}\int_{\partial V_{ij}}\frac{(q-c_i(k))(q-p_i(k))^T\phi(q,k)}{\|p_i(k)-p_j(k)\|}dq, \quad (16)$$

$$\dot{c}_i(k)=\frac{1}{m_i(k)}\int_{V_i(k)}(q-c_i(k))\frac{\partial\phi(q,k)}{\partial k}dq, \quad (17)$$

where $l\in\mathcal{N}_i(k)$, $j\in\mathcal{N}_i(k)\cup\{i\}$, and $\partial V_{i\star}$ denotes the bisectors between Voronoi cell i and an adjacent cell $\star$.

C. Prioritized Response of Newly Emerging Lesions

While existing lesions are healing, new lesions are still emerging before the membrane fully recovers. As these nascent lesions have yet to progress to deeper stages, prioritizing their treatment is essential for controlling the overall lesion burden and preventing further spread. To this end, we develop a strategy that guides microrobots to the centers of newly detected lesions for targeted drug release.

In the absence of new lesions, the CoP distribution shows a continuously non-increasing pattern as a result of drug release. To identify the centers of newly emerging lesions using the updated CoP information, it is essential to delineate the membrane areas impacted by these lesions. However, if the CoP at specific points increases at any given time, these points will be classified as influenced by new lesions. The following assumption is thus made for further discussions.

Assumption 2. *The speed v of the microrobots is significantly higher than the CoP's diffusion rate $\partial\phi(q,k)/\partial k$.*

Therefore, the two control strategies can essentially be executed independently and asynchronously. In other words, when applying the control strategy presented in this section, the Voronoi tessellation at the previous time step can be considered frozen (see Fig. 2). Consequently, the set of points evaluated by the i^{th} microrobot remains confined to its Voronoi cell from before the control strategy transition.

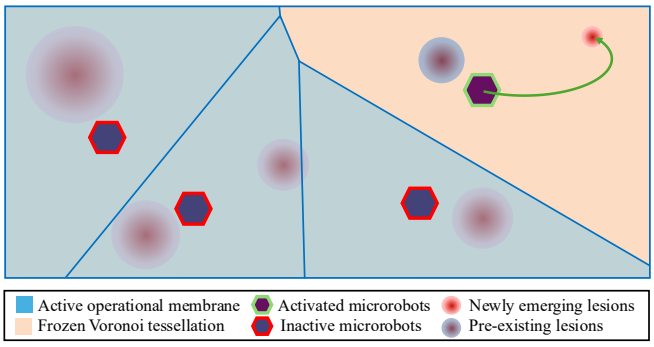

Fig. 2: MRS task execution in frozen Voronoi configuration.

In practice, the sustaining effects of the drug on the membrane actively depress pathogen proliferation. As a result, each microrobot will detect only a small number of new lesions. By selecting a sufficiently small iteration interval T_s, newly emerging lesions can be regarded as appearing sequentially rather than simultaneously. Thus, it is sufficient to consider the characteristics of individual new lesions at each iteration. Accordingly, we define $O_i(k)$ as the region affected by all new lesions detected by the i^{th} microrobot:

$$O_i(k)=\{q:\phi(q,k)>\phi(q,k-1)\geq\mu, q\in V_i(k)\}. \quad (18)$$

It is essential to specify the boundaries of new lesions to distinguish them from others. We begin by defining the neighborhood of a point $q\in V_i(k)$ as the set of its neighbors:

$$\mathcal{N}_q(k)=\{q':\forall\varepsilon_1>0,\exists q', \|q-q'\|<\varepsilon_1\}. \quad (19)$$

Then the boundary of all new lesions is defined as:

$$\partial O_i(k)=\{q':\forall\varepsilon_2>0,\exists q'\in\mathcal{N}_q(k), \|q-q'\|<\varepsilon_2, \phi(q',k)=\mu, q\in O_i(k)\}. \quad (20)$$

Since the boundary of a single lesion is roughly circular, we represent it using the parametric equation $c_x(y)$, where $y\in[0,2\pi]$ and $c_x(0)=c_x(2\pi)$. Let $Z_{i,x}(k)$ denote the affected region by the x^{th} new lesion detected by the i^{th} microrobot. The boundary of $Z_{i,x}(k)$ is defined as follows:

$$\partial Z_{i,x}(k)=\{q':\forall\varepsilon_3>0,\exists q'\in\partial O_i(k),\exists q\in c_x(y), \|q-q'\|<\varepsilon_3\}, \quad (21)$$

where ε_1, ε_2, and ε_3 represent very small positive constants. Thus, the affected region of x^{th} new lesion is given by:

$$Z_{i,x}(k)=\{q:\exists y=c_x^{-1}(q), c_x(y)<0, q\in O_i(k)\}. \quad (22)$$

Our goal is to locate the centers $s_{i,x}\in Z_{i,x}(k)$ of the x^{th} new lesions detected by the i^{th} microrobot. To this end, we formulate a cost function that quantifies the total contribution of newly emerging lesions to the overall CoP:

$$\mathcal{H}_2(P(k),k)=\sum_{i=1}^{I}\sum_{x=1}^{X_i}g(q,s_{i,x}), \quad (23)$$

where X_i is the total number of new lesions discovered by the i^{th} microrobot at k, and $N(k)=N(0)+\sum_{i=1}^{I}X_i$. As noted above, $X_i=1$ when T_s is sufficiently small.

To identify $s_{i,x}$, we optimize $\mathcal{H}_2(P(k),k)$ via a gradient-based approach, where we compute $\partial\mathcal{H}_2(P(k),k)/\partial p_i(k)$. Then the corresponding control law is derived as follows:

$$u_i^{\text{g}}(k)=-\kappa^{\text{g}}(p_i(k)-s_{i,x}), \quad (24)$$

where $\kappa^{\text{g}}=0.5\sigma_{i,x}^{-2}(k)g(q,s_{i,x})$ denotes the mass of the new lesions, which is used as a control gain.

Remark 1. *When a new lesion spans multiple Voronoi cells, i.e., $O_i(k)=Z_{i,x}(k)\cap V_i(t)\neq Z_{i,x}(k)$, a single microrobot cannot delineate the entire lesion based on* (22)*. In such cases, microrobots aggregate data by exchanging information with neighbors to facilitate accurate identification. For the i^{th} microrobot, when $\phi(q\in\partial V_i(k),k)\neq 0$, MRS merges $O_i(k)$ into a new set, regarded as a completely new lesion. Subsequently, each microrobot computes the location of the maximum gradient of the CoP within the portion of the new lesion inside its Voronoi cell as a candidate center $s_{i,x}^{can}=\arg\max_q\phi(q,k)$, where $q\in O_i(k)$. Finally, the position with the globally highest gradient among all candidates is selected as the target location: $s_{i,x}=\arg\max_{s_{i,x}^{can}}\phi(s_{i,x}^{can},k)$.*

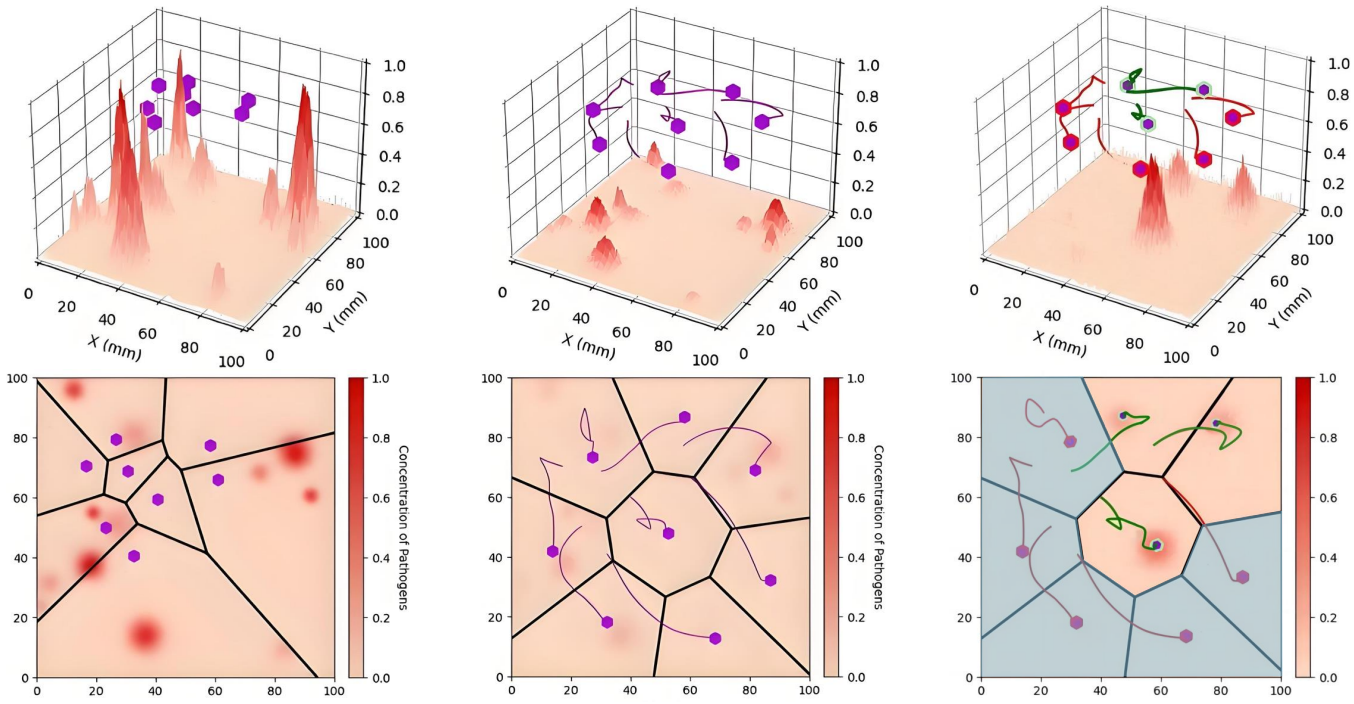

(a) Time=0min (b) Time=65min (c) Time=150min

Fig. 3: Illustration of the evolving microrobot swarm detecting and treating membrane lesions.

D. Event-Triggered Control Strategy

Initially, at iteration $k = 0$, the MRS generates an initial Voronoi configuration based on $P(0)$. At each time step, each microrobot detects the CoP value $\phi(q, k)$ within its corresponding Voronoi cell $V_i(k)$, and compares it with the previous value $\phi(q, k-1)$. This comparison serves as an event-triggering condition that determines which of the following two control laws is implemented at iteration k:

$$u_i(k) = \begin{cases} u_i^{\mathrm{v}}(k) & \phi(q,k) \le \phi(q,k-1) \\ u_i^{\mathrm{g}}(k) & \phi(q,k) > \phi(q,k-1) \end{cases} \tag{25}$$

When $\phi(q, k) \le \phi(q, k-1)$, each microrobot calculates the intermediate terms in (14)-(17), applies the control law (13), and updates its position according to (5). Then it releases the drugs and forms a new Voronoi configuration.

In contrast, when $\phi(q, k) > \phi(q, k-1)$, the microrobot switches to the new lesion response control of (24), which initiates a focused localization process. The i^{th} microrobot identifies the impact range of the new lesion based on (18)-(22). Then we maximize equation (23) and the derived control law (24) navigates the microrobots along the gradient ascent direction towards the center of the new lesion.

Our event-triggered control strategy determines whether to take action based on the detection of new lesions. Instead of keeping the controller continuously active at predetermined time intervals, it issues commands only when a new lesion is identified. This approach relies on a frozen Voronoi partitioning scheme that operates in an essentially asynchronous manner. Such a mechanism avoids unnecessary control actions and thereby reduces resource consumption.

IV. Simulation Results

The membrane to be explored by microrobots is modeled as a finite convex region $\mathcal{Q}$, which is defined by the boundary coordinates $(0, 0), (0, 100), (100, 100), (100, 0)$mm. This region is then discretized using a uniform grid, and the spatial resolution is 0.1 mm. Then our simulation is conducted with a fixed time step of $T_s = 1$ minute.

Lesions are characterized by their oncentration of pathogens (CoP), each represented by a Gaussian function (2). At the initial iteration, 12 lesions are randomly distributed across the membrane. The subsequent emergence of new lesions follows the Hawkes process described in (4), with $\psi(s_n, k) = 0.03$, $\alpha = 0.2$, and $\rho = 0.01$.

Eight microrobots are initially placed at random locations on the membrane. They have a maximum linear velocity of 30 mm/min. Their detection and treatment capabilities are given by (6), with $\delta = 1$ and $\lambda = 0.8$. The control gains are set as $\kappa^{\mathrm{v}} = 0.6$ and $\kappa^{\mathrm{g}} = 1$. Their real-time deployment and motion, governed by (5) and (25), are illustrated in Fig. 3. At $k = 0$, several unrecognized lesions of varying severity are present in the background. As microrobots are dynamically deployed, the red lesion regions progressively fade to flesh tone at $k = 60$, illustrating a monotonic decrease in the CoP. When no new lesions are detected, all robots remain at the centroids of their Voronoi cells for routine monitoring. Once the triggering condition is met at $k = 150$, only the nearest microrobot is activated and directed toward the new lesion, while the others remain stationary. The resulting trajectories demonstrate distinct switching behaviors, underscoring the efficacy of the event-triggered control mechanism.

The treatment efficiency of the proposed strategy is compared with that of the CVT baseline across three key metrics, with results averaged over 100 simulation runs and summarized in TABLE I. Specifically, the proposed strategy reduces new lesion treatment time by 48.7% and shortens total treatment time by 31.9%, demonstrating significant advantages in enabling timely, efficient treatment.

TABLE I: Performance comparison.

Index	Proposed	CVT	Change
New lesions treatment time	90.42	176.17	$\downarrow$ 48.7%
Total treatment time	182.57	268.32	$\downarrow$ 31.9%
Cumulative microrobot activations	13	24	$\downarrow$ 45.8%

Cumulative microrobot activation represents the total number of instantaneous activation events triggered when robots encounter new lesions during operation, manifested as spike signals in tracking error curves. Fig. 4 illustrates that when new lesions arise, our control strategy optimizes braking actions from 8 robots to only 3 robots at $k = 85$, reducing cumulative microrobot activations by 45.8%, ultimately decreasing energy consumption with enhanced performance.

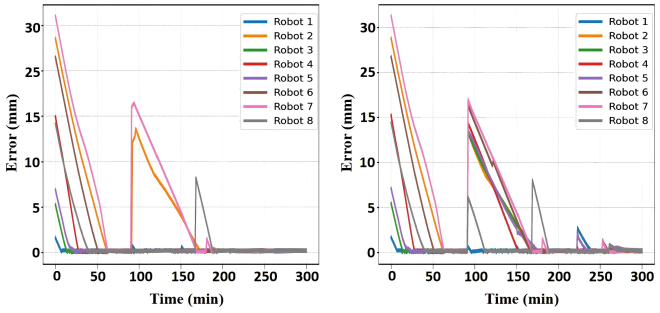

(a) Proposed strategy (b) CVT

Fig. 4: Position error of microrobots under two control strategies.

Under ethical oversight, we will conduct experiments on animals with membrane damage to validate autonomous MRS therapy. Drug-loaded, self-propelled MRS will be endoscopically deployed to target membranes; real-time imaging and fluorescence will track pathological changes and pharmaceutical distribution. Event-triggered coordination will adapt swarm behaviors to evolving micro environments. A randomized, controlled trial will benchmark these systems against conventional delivery on wound-healing rate, drug coverage, and response to new lesions, yielding pivotal safety and efficacy data for clinical translation.

V. Conclusion

In this work, we have developed an event-triggered control framework enabling autonomous detection and targeted treatment of membrane lesions using MRSs. By integrating a lesion model based on reaction-diffusion equations and Hawkes processes, we enhanced the Lloyd algorithm for improved spatial coverage and drug delivery precision. Additionally, the event-triggered control strategy ensures a timely response to newly emerging lesions, dynamically reallocating microrobot resources to suppress proliferation and promote effective healing. Simulation results validate the method's performance, demonstrating significant reductions in total treatment duration compared to traditional methods. Future work will focus on extending the framework to more complex microrobot dynamics and validating the approach with clinical lesion datasets and experimental trials.

References

[1] M. Sitti, H. Ceylan, W. Hu, J. Giltinan, M. Turan, S. Yim, and E. Diller, "Biomedical applications of untethered mobile milli/microrobots," *Proceedings of the IEEE*, vol. 103, no. 2, pp. 205–224, 2015.

[2] J. Yu, D. Jin, K.-F. Chan, Q. Wang, K. Yuan, and L. Zhang, "Active generation and magnetic actuation of microrobotic swarms in bio-fluids," *Nature Communications*, vol. 10, no. 1, p. 5631, 2019.

[3] L. Yang, J. Yu, S. Yang, B. Wang, B. J. Nelson, and L. Zhang, "A survey on swarm microrobotics," *IEEE Transactions on Robotics*, vol. 38, no. 3, pp. 1531–1551, 2021.

[4] V. Agrahari, V. Agrahari, M.-L. Chou, C. H. Chew, J. Noll, and T. Burnouf, "Intelligent micro-/nanorobots as drug and cell carrier devices for biomedical therapeutic advancement: Promising development opportunities and translational challenges," *Biomaterials*, vol. 260, p. 120163, 2020.

[5] J. Li, B. Esteban-Fernández de Ávila, W. Gao, L. Zhang, and J. Wang, "Micro/nanorobots for biomedicine: Delivery, surgery, sensing, and detoxification," *Science Robotics*, vol. 2, no. 4, p. eaam6431, 2017.

[6] W. Waddingham, U. Kamran, B. Kumar, N. J. Trudgill, Z. P. Tsiamoulos, and M. Banks, "Complications of diagnostic upper gastrointestinal endoscopy: common and rare–recognition, assessment and management," *BMJ Open Gastroenterology*, vol. 9, no. 1, p. e000688, 2022.

[7] M. Zhang, J. Liang, Y. Yang, H. Liang, H. Jia, and D. Li, "Current trends of targeted drug delivery for oral cancer therapy," *Frontiers in bioengineering and biotechnology*, vol. 8, p. 618931, 2020.

[8] Y. Ilan, "Overcoming compensatory mechanisms toward chronic drug administration to ensure long-term, sustainable beneficial effects," *Molecular Therapy Methods & Clinical Development*, vol. 18, pp. 335–344, 2020.

[9] J. G. Lee, R. R. Raj, N. B. Day, and C. W. Shields IV, "Microrobots for biomedicine: unsolved challenges and opportunities for translation," *ACS Nano*, vol. 17, no. 15, pp. 14196–14204, 2023.

[10] Y. Wang, J. Shen, S. Handschuh-Wang, M. Qiu, S. Du, and B. Wang, "Microrobots for targeted delivery and therapy in digestive system," *ACS Nano*, vol. 17, no. 1, pp. 27–50, 2022.

[11] L. Yang, J. Jiang, F. Ji, Y. Li, K.-L. Yung, A. Ferreira, and L. Zhang, "Machine learning for micro-and nanorobots," *Nature Machine Intelligence*, vol. 6, no. 6, pp. 605–618, 2024.

[12] Q.-L. Han, L. Ding, and X. Ge, "Special issue on event-triggered control and filtering of distributed networked systems," *IEEE Transactions on Systems, Man, and Cybernetics: Systems*, vol. 50, no. 9, pp. 3108–3111, 2020.

[13] Y. Sun, Z. Ji, Y. Shi, and Y. Liu, "Event-based finite time stabilizability and formation control of multi-agent systems," *IEEE Transactions on Automation Science and Engineering*, vol. 22, pp. 7887–7896, 2024.

[14] Z. Wang, S. Piao, Y. Ji, X. Wang, and F. Tsung, "An efficient dual-observer method for leader-following consensus control of multiagent systems," *IEEE 21st International Conference on Automation Science and Engineering*, 2025.

[15] Y. Gao, Z. Zhou, H. Gao, S. Zhang, and Y. Ji, "Switch control for robot swarms to detect critical nodes in heterogeneous sensor networks," in *IEEE 21st International Conference on Automation Science and Engineering*, 2025.

[16] J. Cortes, S. Martinez, T. Karatas, and F. Bullo, "Coverage control for mobile sensing networks," *IEEE Transactions on Robotics and Automation*, vol. 20, no. 2, pp. 243–255, 2004.

[17] B. Şenbaşlar and G. S. Sukhatme, "Asynchronous real-time decentralized multi-robot trajectory planning," in *IEEE/RSJ International Conference on Intelligent Robots and Systems*, pp. 9972–9979, 2022.

[18] Y. Gao, K. Luo, C. Fang, and J. He, "Fragility-aware stealthy attack strategy for multi-robot systems against multi-hop wireless networks," in *61st IEEE Conf. on Decision and Control*, pp. 4827–4832, 2022.

[19] S. Zhuang, G. Zhang, D. Lei, X. Yu, M. Tong, W. Lin, Y. Shi, and H. Gao, *Robotic Micromanipulation of Zebrafish Larva*. Springer, 2023.

[20] R. Lin and M. Egerstedt, "Predator-prey interactions through heterogeneous coverage control using reaction-diffusion processes," in *62nd IEEE Conference on Decision and Control*, pp. 5431–5436, 2023.